Research Square

Preprints are preliminary reports that have not undergone peer review.
They should not be considered conclusive, used to inform clinical practice,
or referenced by the media as validated information.

Thermogenic stimulation with a β3-adrenergic receptor agonist prevents the cold- induced rise of phosphorylated tau in a mouse model of Alzheimer's disease

Josue Valentin-Escalera
Université Laval
Hélèna Denis
Centre de recherche du CHU de Québec-Université Laval
Paul Pillet
Université Laval
Marine Tournissac
Université Laval
Cyntia Tremblay
Centre de recherche du CHU de Québec-Université Laval
Vincent Émond
Centre de recherche du CHU de Québec-Université Laval
Sébastien S. Hébert
Université Laval
Emmanuel Planel
Université Laval
Frédéric Calon
Frederic.Calon@pha.ulaval.ca

Université Laval

Research Article

Keywords: Alzheimer's disease, cold exposure, β3-AR agonist, 3xTg-AD mice, thermogenesis, hyperphosphorylated tau, plasma pTau-217

Posted Date: August 27th, 2026

DOI: https://doi.org/10.21203/rs.3.rs-10436119/v1

License: This work is licensed under a Creative Commons Attribution 4.0 International License.
Read Full License

Additional Declarations: No competing interests reported.

Abstract

Background: Alzheimer's disease (AD) is an age-related brain disorder associated with metabolic and thermoregulatory deficits. Here, we tested whether enhancing thermogenesis through pharmacological stimulation of brown adipose tissue (BAT) with a β3-adrenergic receptor (β3-AR) agonist can protect against cold-induced tau phosphorylation in a mouse model of AD neuropathology.

Methods: A b3-AR agonist (CL-316,243) was administered to old (18 months), male 3xTg-AD and NonTg mice for 4 weeks at a dose of 1 $mg.kg^{-1}.day^{-1}$ i.p. Mice were then subjected to an acute cold exposure (4°C) during 24h, to enhance tau hyperphosphorylation. A group of saline-treated mice was kept at room temperature (22°C) as controls.

Results: Chronic administration of b3-AR agonist induced weight loss, improved peripheral glucose and insulin metabolism, enhanced thermogenesis and modulated FGF21 in both NonTg and 3xTg-AD mice. While b3-AR agonist treatment slightly decreased the ratio of soluble Ab42/Ab40 in the cortex, it almost completely blunted the cold-induced soluble tau hyperphosphorylation (pTau) in the hippocampus of 3xTg-AD mice. Acute cold exposure also led to the detection of pTau-217 in the plasma, which was attenuated by β3-AR stimulation.

Conclusions: Our results indicate that BAT stimulation through pharmacological activation of b3-AR protected against cold-induced tau hyperphosphorylation and attenuated Ab pathology in 18-month-old 3xTg-AD mice. Treatment with a b3-AR agonist could represent a therapeutic strategy in AD by counteracting both metabolic deficits and neuropathology.

Background

Aging is the most prominent risk factor for Alzheimer's disease (AD), which is characterized by the accumulation of neurofibrillary tangles (NFTs) and β-amyloid (Aβ) plaques in the brain (1–3). Among the key physiological changes associated with advanced age, impairments in thermoregulation are commonly observed. This decline in the ability to maintain body temperature coincides with the sharp rise in the incidence of AD (4–7).

Clinical studies have associated core body temperature and cognitive status (8–10). Recent clinical data suggest that changes in body temperature affect cognition and pTau dynamics in the brain. Individual-based hypothermia index as measured by wireless devices has been associated with impaired memory function, while post-wake body temperature variations positively correlate with CSF and plasma pTau (9, 11, 12).

A wealth of preclinical research has taught us that body temperature changes are one of the strongest modulators of the phosphorylation of tau (pTau), the primary component of NFTs (9, 12–15). Hypothermia invariably leads to a higher proportion of pTau at several key epitopes in the brain of rodents and hibernating animals (16–21). Conversely, a thermoneutral environment or normothermia

rather promotes cerebral tau dephosphorylation in animals (14, 16, 18). However, these approaches are not only difficult to implement in clinical settings, but they also fail to correct the central cause of thermoregulatory deficits. Given the experimental evidence linking advanced age, body temperature, and tau phosphorylation, targeting thermogenesis in elderly individuals emerges as a compelling strategy to potentially modulate the neuropathological processes underlying AD.

The discovery of active brown adipose tissue (BAT) in adults has opened the door to strategies to enhance non-shivering thermogenesis (NST) (22–26). Our recent studies conducted on the 3xTg-AD animal model have shown that stimulating BAT, through either pharmacological or non-pharmacological approaches, can correct metabolic deficits and improve AD neuropathology. One way to achieve this involves BAT “training” to respond to thermal challenges through repeated short-cold exposures (RSCE; 4°C, 4h, 5 days/ week). This non-pharmacological approach has been shown to improve glucose metabolism and protect against the cold-induced rise of pTau in the hippocampus (17). By taking advantage of the selective localization of β3-adrenergic receptor (β3-AR) in BAT, selective β3-AR agonists offer a means to pharmacologically stimulate NST (27). We have previously shown that administration of the β3-AR agonist CL316, 243 in 3xTg-AD mice improved memory function and Aβ pathology (28). However, the effect on tau phosphorylation was limited, likely because the agonist was not evaluated under a cold challenge paradigm, precluding any detection of the preventable rise of pTau. Indeed, acute cold exposure is a classical way not only to trigger and study thermogenesis but also to enhance tau phosphorylation (14, 18, 29). Therefore, in this study, we investigated whether chronic activation of thermogenesis through a β3-AR agonist could improve metabolic function and AD-like neuropathological markers in cold-challenged 3xTg-AD mice. Since tau hyperphosphorylation is recognized as both a key biomarker and a major therapeutic target in AD (30–33), we focused our efforts on measuring this parameter in the brain and the periphery.

Methods

Animals

The triple-transgenic mouse model of Alzheimer’s disease (3xTg-AD; homozygous APPswe, PS1 M146V, and tau P301L), which develops both amyloid-β and tau neuropathology, was used in this study and compared with non-transgenic (NonTg) controls sharing the same mixed C57BL6/129Svj genetic background. This model is well suited to study AD-associated thermoregulatory impairments, as we have previously shown that 3xTg-AD mice exhibit deficits in body temperature regulation that closely parallel the development of AD-like neuropathology (14, 17, 28). Animals were bred in-house and maintained on a stable genetic background by backcrossing every 8–10 generations.

In total, 69 male 3xTg-AD and NonTg mice aged 18 months (SEM ± 0.2 months) at the beginning of the protocol were used for all experiments. Mice were housed in groups of one to five per cage under controlled environmental conditions (22 ± 2°C) and a 12:12-h light–dark cycle (lights on from 7:00 a.m. to 7:00 p.m.), with ad libitum access to water and standard chow (Teklad 2018, Harlan Laboratories,

Canada). Only males were included to ensure consistency with data generated in our previous studies using this methodological approach (13, 16, 25) and to minimize variability in body temperature and sleep–wake regulation associated with sex hormones and the estrous cycle, which have been shown to influence thermoregulation in a sex-dependent manner (34, 35). This approach was also chosen because of the logistical and ethical challenges associated with exposing large numbers of animals to cold in our facilities. All experimental procedures were conducted in accordance with the guidelines of the Canadian Council on Animal Care and were approved by the Institutional Committee for Animal Care of the Centre Hospitalier de l'Université Laval (CHUL).

CL-316,243 treatment and cold exposure

Mice were injected with the β3-AR agonist CL-316,243 (1mg/ kg, i.p.), for one month (28 consecutive injections) as previously described (28). After the final injection, a group of saline-injected mice and the β3-AR agonist treated group were exposed to an acute cold challenge at 4°C for 24h (acute cold-exposed group) (Fig. 1A). An additional group of saline-injected mice was kept at housing temperature 22 ± 2°C during the 1-month treatment to control for treatment and temperature effects. Mice in the cold-exposed groups were housed individually to prevent mutual warming during the 24-h cold exposure challenge and assess thermoregulatory capacity. After, mice were anesthetized at their respective temperatures as previously described (17).

Body temperature measurement

Telemetry-based measurements were previously utilized by our group to show that CL-316,243 treatment increased body temperature during the light-phase of the light-dark cycle (28). To minimize logistical constraints associated with surgery, two alternative, less invasive methods were used to monitor body temperature. An infrared thermometer (BIO-IRB 153, BIOSEB Lab instruments) was used to measure surface temperature at the tail, while a Thermocouple Meter (MicroTherma 2K High Pecision Type K, ThermoWorks) was used for rectal temperature measurements. Rectal and infrared temperatures were measured on alternating days before each i.p. injection, between 10 am-1pm.

Glucose tolerance and insulin tolerance tests

Glucose tolerance test (GTT) and insulin tolerance test (ITT) were performed starting the third and fourth week of treatment, respectively (Fig. 1A) (36). Mice were fasted for 6h (from 8 a.m. to 2 p.m.). For the GTT, glucose was injected i.p. at 1 g/kg and blood glucose was measured at regular intervals during 2h with a glucometer (OneTouch UltraMini; LifeScan, Milpitas, CA) in a blood drop sampled from the saphenous vein. For the ITT, commercial insulin (Novolin Toronto) was injected i.p. at 1 U/ kg and blood glucose was measured during 1h with the same method.

Tissue preparation for postmortem analysis

At the end of the experimental protocol, mice were deeply anesthetized by intraperitoneal injection of ketamine (100 mg/kg) and xylazine (10 mg/kg) and were rapidly euthanized by intracardiac perfusion with ice-cold 0.1 M phosphate-buffered saline (PBS) supplemented with phosphatase inhibitors (sodium pyrophosphate, 1 mM; sodium fluoride, 50 nM) and protease inhibitors (SigmaFAST™, Sigma-Aldrich, St-Louis, USA). Intracardiac blood sampled in a heparinized tube just before intracardiac perfusion was centrifuged at 3000 rpm for 5 min, and resulting plasma was kept frozen at -80°C until analysis. Although anesthesia affects body temperature (37), all mice were deeply anesthetised before intracardiac perfusion for obvious ethical reasons, but they underwent the same anesthesia regimen and were kept under a heat pad until perfusion. The first hemisphere and interscapular BAT were rapidly dissected and frozen at -80°C until processing. The second entire hemisphere was frozen and kept at -80°C.

Protein extractions

For the hippocampus and cortex, frozen samples were homogenized in 8 volumes of a lysis buffer (150 mM NaCl, 10 mM NaH_2PO_4, 0.5% sodium deoxycholate, 0.5% sodium dodecyl sulfate, 1% Triton X-100) containing a cocktail of protease and phosphatase inhibitors (100X, Selleck Chemicals, Houston, Tx), sonicated (3 x 45 s in a Sonic Dismembrator apparatus, Thermo Fisher Scientific, Waltham, MA) and centrifuged (100,000g, 20 min, 4°C), resulting in a detergent-soluble fraction (cytosolic, extracellular, and membrane-bound proteins). The remaining pellets from ultracentrifugation were resuspended in formic acid, resulting in a detergent-insoluble fraction (insoluble protein fraction). The resultant suspension was sonicated and centrifuged (13,000 g, 20 min, 4°C), acid formic was evaporated and proteins were either solubilized in Laemmli's buffer for Western blot or in 5 M guanidium solution in Tris-HCL 50 mM for Aβ peptide ELISAs (see below), as previously described (32). Because of its small size, proteins from the BAT were extracted in the lysis buffer only. Protein concentrations were evaluated with a bicinchoninic acid assay (BCA, Pierce, Rockford, IL, USA).

Western immunoblotting

In total, 10–15 µg of proteins of hippocampus, cortex and BAT homogenates were loaded and separated by SDS-PAGE, as previously described (1, 14, 38). The list of antibodies used in this study is available in additional file 1. For each experiment, all homogenates were run on the same gel. Membranes were imaged using the Amersham Imager 680 (Cytiva). Quantification was performed using the ImageLab software (Millipore) and results were expressed as relative optical densities (OD). For the analysis of the protein tau, all isoform bands detected around 60 kDa were quantified together.

RT-qPCR of Ucp1 and Fgf21

The expression levels of uncoupling protein 1 (*Ucp1*, TaqMan Gene Expression Assays, Mm01244861_m1, Life Technologies), *Fgf21* (TaqMan Gene Expression Assays, Mm00840165_g1, Life Technologies) and β2-microglobulin (*β2m*, Mm00437762_m1, Life Technologies) mRNA were determined in BAT using a reverse transcription real-time quantitative PCR (RT-qPCR), as previously described (18). The delta delta Ct (ddCT) method was used to evaluate differences in relative gene expression between groups using β2m as the control gene. Results are presented as ratios of *Ucp1/ β2m* or *fgf21/ β2m* cDNA relative to the control group.

Aβ40 and Aβ42 ELISA

Aβ peptides were quantified in protein extracts from the cortex. Aβ40 and Aβ42 were measured in TBS-soluble and detergent-insoluble fractions using a human highly sensitive amyloid-β ELISA (Wako, Osaka, Japan) according to the manufacturer´s instructions. Plates were read at 450 nm using a Synergy™ HT multi-detection microplate reader (Biotek, Winooski, VT).

FGF21

Levels of FGF21 was determined in plasma sampled before intracardiac perfusion in non-fasted mice using the mouse/rat FGF21 Quantikine ELISA kit (MF2100, R&D systems, Minneapolis, MN). Plates were read at 450 nm using a Synergy™ HT multi-detection microplate reader (Biotek, Winooski, VT).

Plasma pThr-217 ELISA

Levels of human pThr-217 were determined in plasma samples according to kits instructions using the S-PLEX Human Tau (pT217) kit number K151APFS-2, Meso Scale Diagnostics, 1601 Research boulevard, Rockville Maryland US. For most 3xTg-AD animals kept at room temperature, a signal was detected just below the linear range of the standard curve.

Statistical analysis

Data are represented as means ± standard error of the mean (SEM). Statistical analysis and the number of samples per group are specified in each figure and the legend. Barlett’s test was used to assess homogeneity of variances between the groups. Repeated measures mixed-effect model was used to analyzed recurrent temperature measurements and body weight changes in same animals during the 1-month treatment. To determine the effect of genotype and agonist treatment before cold exposure, two-way ANOVAs (genotype x treatment) were performed in case of equal variances, followed by Šidák´s post-hoc multiple comparison. For pTau and other data including the two genotypes (NonTg, 3xTg-AD) and three experimental conditions (saline 22°C, saline 4°C, agonist 4°C) a standard least squares model was performed where genotype and the three conditions were included as fixed effects, followed by a Dunnett’s post-hoc test. In addition, as a secondary conservative approach given the small sample sizes, to probe for group differences in NonTg and 3xTg-AD mice exposed to cold and agonist pretreatment, while minimizing assumptions of normality or equal variances, we also performed a Kruskal–Wallis analysis followed by Wilcoxon’s post-hoc test. Correlations between variables were investigated using

linear regression analyses. A ROUT test was performed to test for outliers (as indicated in legends). For categorical data, a Fisher's exact test was used determine statistical significance. All statistical analyses were performed with Prism 10 (GraphPad Software Inc., San Diego, CA, USA) or JMP (Version 18; SAS Institute Inc., Cary, IL., USA) software and statistical significance was set at p = 0.05.

Results

One-month β3-AR agonist treatment results in weight loss and improves glucose metabolism in aged mice

NonTg and 3xTg-AD mice were injected daily (i.p.) with saline or a β3AR agonist (CL-316,243 at a dose of 1 mg/ kg i.p.) for one month (Fig. 1A). To assess the effect of β3-AR stimulation on peripheral metabolism in old mice, mice were weighed once per week during treatment and metabolic tests were performed following the third week of injections. As expected, at the end of treatment, we observed that chronic injection of the β3-AR agonist induced a total weight loss in NonTg and 3xTg-AD mice (mean ± SEM = -10.2% ± 1.9 and − 7.7% ± 2.0, respectively) compared to saline-treated mice (mean ± SEM = -2.6% ± 0.8 and − 4.0% ± 0.6, respectively) (Fig. 1B). As we have shown previously (28), glucose (GTT) and insulin tolerance tests (ITT) revealed that the β3-AR agonist-treated mice displayed lower fasting glucose after three weeks of treatment (Fig. 1C), while exerting a better control over glucose and insulin metabolism (Fig. 1D, F, **and E, G** for AUC statistical comparison). Overall, our data confirm that chronic pharmacological stimulation of β3-AR improves metabolic determinants in NonTg and 3xTg-AD mice at 18 months of age.

Chronic β3-AR stimulation followed by acute cold exposure increases thermogenesis in NonTg and 3xTg-AD mice

During the 4-week treatment with CL-316,243, we recorded rectal and infrared (IR) temperatures on alternating days, before each injection. Repeated measures mixed-effect model analyses and AUC comparisons revealed an increasing effect of CL-316,243 treatment in the % change in rectal and IR tail temperatures, using NonTg mice on saline as a baseline of comparison (Fig. 2A-C). In addition, the changes in temperature during the duration of the treatment were slightly more pronounced in 3xTg-AD mice (genotype effect, *p < 0.05) (Fig. 2A, B). Consistent with previous reports (28, 39), these data confirm the capacity of CL-316,243 to increase body temperature in mice kept at RT.

β3-AR stimulation leads to thermogenesis via activation of UCP1, which is abundantly expressed in BAT (40). To confirm target engagement, we assessed UCP1 levels (mRNA) in BAT homogenates. Higher expression levels of *ucp1* mRNA were seen following acute cold exposure compared to mice at RT. However, the rise of *ucp1* was not significant due to high variability in saline-injected 3xTg-AD mice (Fig. 2D). Pretreatment with CL-316,243 had a slightly additive effect, resulting in significantly increased

ucp1 mRNA in agonist-treated mice 3xTg-AD mice versus controls (Fig. 2D). Although chronic stimulation with CL-316,243 have been reported to downregulate relative levels of the β3-AR in BAT (28, 41), we did not observe any change after one month treatment (Fig. 2E). Lastly, we measured the relative levels of mitochondrial oxidative phosphorylation complexes I to V (OXPHOS system) as an index of mitochondrial respiratory and thermogenic capacity (28, 42). β3-AR agonist treatment increased complex I (NADH: Ubiquinone oxidoreductase), with a significant difference between saline-treated (4°C) and agonist-treated (4°C) mice (Fig. 2F). The rest of the OXPHOS system remained unchanged with either acute cold exposure or agonist treatment (Fig. 2. **G-J**). In all, these data confirmed that pharmacological administration of CL-316,243 enhances BAT thermogenesis, on top of acute cold exposure, in 18-month-old NonTg and 3xTg-AD mice.

Cold exposure upregulates fgf21 in BAT and FGF21 in the plasma while β-3AR stimulation lowers the proportion of activated FGFR1

Thermogenic activation of BAT not only induces UCP1-dependent heat production but also triggers the release of batokines, including the fibroblast growth factor-21 (FGF21) (24). Hence, we questioned if acute cold exposure (4°C, 24h) and pharmacological β3-AR stimulation modulated FGF21 in BAT homogenates and in circulation. While we did not detect significant changes on FGF21 protein levels with either acute cold or agonist treatment in BAT, cold exposure significantly increased *fgf21* gene expression in BAT, which was prevented by chronic β3-AR activation (Fig. 3A, B). Intriguingly, the $pFGFR1_{(Y653/654)}$/ FGFR1 ratio in the BAT was not increased by cold exposure but rather reduced by the agonist pretreatment (Fig. 3C). In parallel, plasma FGF21 concentrations increased following acute cold exposure, an effect blocked by chronic pharmacological BAT activation (Fig. 3D). However, differences in plasma FGF21 reached statistical significance only in NonTg mice, suggesting a partially blunted FGF21 response in 3xTg-AD mice. Activation of FGFR1 in BAT (indexed with the pFGFR1/FGFR1 ratio) was strongly correlated with circulating plasma FGF21 levels, further supporting BAT as a physiological target of this metabolic hormone (Fig. 3E). In sum, these results show that cold exposure induces BAT to produce and secrete FGF21, which subsequently activates its receptor, and that these effects are prevented by pretreatment with a β3-AR agonist.

β3-AR stimulation maintains soluble Aβ42/Aβ40 ratio at control levels in cold-exposed 3xTg-AD mice

We next evaluated if cold exposure and β3-AR stimulation modified levels of Aβ40 and Aβ42 in soluble and insoluble cortex homogenates of 3xTg-AD mice. In both, TBS-soluble and insoluble fractions, cold exposure did not change significantly the levels of Aβ40 and Aβ42 peptides. However, although the cold exposure–induced increase in the Aβ42/Aβ40 ratio (28%) did not reach statistical significance, treatment with the agonist preserved this ratio at control levels (− 25%) (Fig. 4C). In the insoluble fraction, there was a similar tendency (although not significant, $p = 0.06$) to cold-induced rise in Aβ42/Aβ40 (+ 75%), but that was not altered by the agonist pre-treatment (Fig. 4F). Relative levels of β-site amyloid precursor protein cleaving enzyme 1 (BACE-1, involved in Aβ production) and insulin

degrading enzyme (IDE, involved in Aβ clearance) also remained unchanged between groups (Fig. 4G, H). Of note, mitochondrial NADH-ubiquinone oxidoreductase (Complex I; CI) levels correlated negatively with the ratio of soluble Aβ42/40, and circulating FGF21 correlated negatively with insoluble Aβ42 (Fig. 4J, K), suggesting an inverse relationship between BAT activity and Aβ pathology, while this is not found for pTau (Additional file 2. Table 1). Overall, these results indicate that sustained BAT thermogenesis may exert beneficial effects on Aβ pathology by maintaining the soluble Aβ42/40 ratio at control levels during cold exposure.

β3-AR stimulation prevents the cold-induced rise of hippocampal pTau

To measure if the β3-AR agonist prevented the rise of hypothermia-induced tau phosphorylation, we exposed the mice to acute cold (4°C, 24h) before euthanasia. The phosphorylation status of tau was quantified by Western blot at several key epitopes, expressed as ratios over total tau, in both the soluble (enriched in cytosolic proteins, Fig. 5) and detergent-insoluble (enriched in aggregates, Additional file 2. Figure. 1) fractions.

As expected, these experiments first showed that acute cold increased soluble pTau at four different epitopes in hippocampal homogenates of NonTg and 3xTg-AD mice: pThr217 (polyclonal): +212% and + 52%; pSer202 (CP13): +170% and + 64%; pSer396/404 (PHF-1): +100% and + 75%: pSer202/Thr205 (AT8): +145% and 139% vs non-exposed NonTg and 3xTg-AD mice, respectively (Fig. 5A-D).

Pretreatment with the β3-AR agonist prevented the rises in pTau at all these epitopes, except for AT8 (pSer202/Thr205). These effects were particularly striking in 3xTg-AD mice where the agonist kept pTau at levels similar to non-exposed controls (pThr217: -45%; CP13 (pSer202): -35%; and PHF-1 (pSer396/404): -36% but not in NonTg mice (Fig. 5A-D). Neither cold exposure nor CL316,243 had significant impact on pThr181 tau (AT270) or total tau (Tau C for mouse+human tau or Tau 13 for human tau), although, as expected, 3xTg-AD displayed more of phosphorylated, total and human tau than NonTg mice (Fig. 5E-G). In the detergent-insoluble fraction, the effects of cold exposure on tau phosphorylation and the protective effect of the agonist were detectable only at CP13 (pSer202), indicating a much-attenuated effect of treatments in aggregated tau (Additional file 2. Figure 1). In addition, the changes in soluble pTau could not be explained by alterations in GSK3β, a kinase known to phosphorylate tau at serine 202 and 396, nor by changes in methylated PP2A-C or total PP2A-C (Additional file 2. Figure 2). Overall, these results indicate that sustained thermogenesis achieved with a β3-AR agonist can blunt the physiological increase in soluble tau phosphorylation following exposure to cold.

Cold exposure enables the detection of plasmatic pTau-217, an elevation that is partially blocked by β3-AR agonist pretreatment

We next sought to determine whether circulating pTau (pThr-217) is detectable in aged 3xTg-AD mice, an emerging AD biomarker that correlates with Aβ plaque burden (30, 31), and whether it is modulated by

cold exposure with or without a β3-AR agonist pretreatment. First, as expected, no signal was detected in NonTg mice. In 3xTg-AD mice maintained at room temperature, pTau-217 levels were measurable, above the detection limit, but below the linear range of the standard curve in five out of six animals. Cold exposure significantly increased the number of samples within the linear (quantifiable) range of the standard curve, with 11 out of 13 mice showing pTau217 levels within that range, significantly higher than the non-exposed group, suggesting that hypothermia results in release of pTau217 in the plasma (Fig. 6A, B). Pretreatment with the β3-AR agonist significantly decreased this ratio to 7 out of 13 mice (Fig. 6A, B). Plasma pTau217 also correlated positively with relative levels of insoluble pSer202 (CP13) and pSer396/404 (PHF-1) in the brain cortex, suggesting that peripheral pTau217 reflects increases in brain tau pathology associated with aggregated forms (Fig. 6C, D). These new results indicate that it is possible to detect the tau protein phosphorylated at Threonine 217 (pTau217) in the blood of 3xTg-AD mice, but more reliably after hypothermia, while the β3-AR agonist showed a partial ability to prevent this secretion.

Discussion

Tau hyperphosphorylation in the brain and, more recently in the blood, are the markers most strongly associated with AD symptoms (30–32). As such, they represent particularly promising therapeutic targets, or at the very least, the most useful surrogate markers of neuropathology. This study shows that systemic administration of a β3-AR agonist protects against the cold-induced increase of pTau in the hippocampus of 3xTg-AD mice. Specifically, pretreatment with the β3-AR agonist for four weeks almost completely blunted the rise of soluble pTau at pThr217, CP13 (pSer202) and PHF-1 (pSer396/404), induced by a cold challenge. The observed changes in the brain were accompanied by a similar pattern in plasma pTau217 levels, suggesting that such an intervention could be monitored in vivo in a clinical trial. Treatment with the agonist also resulted in a reduction of the cortical soluble Aβ42/ Aβ40 ratio compared to cold-exposed 3xTg-AD mice. These effects in the brain occurred in parallel with proof of target engagement in the BAT and potent metabolic effects in the periphery of the β3-AR agonist. These results highlight the potential of pharmacologically stimulating key metabolic processes such as thermogenesis to prevent hypothermia-induced accumulation of hallmark neuropathological markers in AD.

β3-AR activation improves thermogenesis and glucose metabolism in old mice

Confirmation of target engagement by β3-AR agonists requires direct assessment of brown adipose tissue (BAT) activation. The molecular signatures of thermogenic capacity in brown adipocytes include the mitochondrial uncoupling protein 1 (UCP1) and complex I (CI) of the electron transport chain. Here, both CI protein and *ucp1* mRNA levels were upregulated after chronically administering CL316,243, indicating sustained thermogenic capacity throughout the treatment period, as previously observed (28,

43). These essential experiments confirm that stimulation of BAT with the β3-AR agonist CL-316,243 is effective in old mice of both genotypes.

It is well accepted that metabolic disturbances in mid-life increase the risk of developing AD (44, 45). This points to the therapeutic potential of addressing metabolic dysfunctions, both systemic and cerebral, as a strategy for modifying AD progression, especially at early stages (46). Following the discovery of active BAT in adult humans (23, 25), preclinical studies evidenced the efficacy of targeting BAT function to improve cardiometabolic health (22, 24). β3-AR agonists have been tested in registered clinical trials (RCTs) for such indications (47, 48), but their efficacy has not matched that of other anti-diabetic or anti-obesity agents, such as GLP-1 receptor agonists, and thus attempts to develop clinically useful agonists in metabolic diseases have faltered (49, 50). Here, we show that the β3-AR agonist significantly improved glucose metabolism and insulin tolerance as seen by the glucose and insulin tolerance tests in NonTg and 3xTg-AD mice. This is in line with previous reports by our group and others where chronic treatment with CL316,243 in aged 3xTg-AD or C57BL/6J mice improved metabolic homeostasis in the periphery (22, 28). These results confirm that aged 3xTg-AD mice respond to β3-AR activation, leading to an overall improved metabolic profile.

β3-AR activation reduces soluble Aβ42/40 ratio in cold-exposed 3xTg-AD mice

Aβ remains a key therapeutic target in AD being tested in several preclinical and clinical trials (33). Beside their diagnostic use, Aβ42 plaques correlate with cognitive symptoms, albeit imperfectly (51, 52). The two anti-Aβ monoclonal antibodies recently approved for therapeutic application in several countries lower PET-estimated Aβ burden, but also reduce plasma pTau217 and slow cognitive decline, representing a major advancement in the field (53, 54). It is noteworthy to mention that assessing the cerebral Aβ42/40 ratio can be a more reliable indicator of pathological β-amyloid processing than absolute levels alone, as it captures the shift toward toxic Aβ42 aggregation, probably at the expense of Aβ40 (55). Virtually all AD-causing mutations on APP and PSEN increase the Aβ42/40 ratio in the brain, which correlate with age-of-onset of clinical manifestations in familial AD (56). In the present study, treatment with CL316, 243 reduced cortical soluble Aβ42/Aβ40 ratio by 25% compared to cold exposed 3xTg-AD mice. Though we did not observe a significant change in the insoluble Aβ42/40 ratio, a previous study from our group reported a 27% decrease in insoluble Aβ42/Aβ40 ratio in the hippocampus of 3xTg-AD mice in slightly younger mice (16-month-old) when treated with the same agonist (28). Other approaches to target thermoregulation including a thermoneutral environment (28°C) reduced insoluble Aβ42 while repeated short-cold exposures (RSCE) had no effect on the Aβ42/40 ratio (14, 17). As β3-AR agonists offer a dual mechanism of action; tackling thermoregulatory and metabolic deficits, repurposing them may prove advantageous in reducing Aβ pathology.

β3-AR agonist treatment confers protection against cold-induced pTau

The 3xTg-AD mouse is one of the very few animal models that exhibit both pTau and Aβ pathologies, as fully formed neurofibrillary tangles and Aβ plaques (57). We employed cold exposure to test hypothermia-related tau phosphorylation mechanisms. The effect of cold exposure seen here confirms the key role of low body temperature as a fundamental contributor to tau hyperphosphorylation (12, 13, 16). As thermogenic deficits become more apparent with age (4–7), tackling thermoregulation can be a valuable strategy to protect the elderly from deleterious hypothermic events (9, 10, 15). Importantly, β3-AR pretreatment conferred full protection against the cold-induced rise of soluble pTau at pThr217 (polyclonal), CP13 (pSer202), and PHF-1 (pSer396/404) in 3xTg-AD mice, with a limited effect on insoluble pTau, suggesting that it enhances thermogenic capacity in old mice, thereby preventing hypothermia and AD-related deleterious effects. A previous report from our team involving the same β3-AR agonist (CL-316,243) found beneficial effects on behaviour, metabolism and β-amyloid pathology, but did not detect any effect on pTau on mice left at room temperature; likely because it was not evaluated under a cold-exposure paradigm (28). Nonetheless, we have previously reported that repeated short cold exposures, a nonpharmacological method to stimulate BAT thermogenesis in the mouse, confer such protection in soluble pTau (17). Both soluble monomeric and oligomeric soluble pTau are considered important drivers of neurotoxicity, especially for their capacity to spread throughout brain regions (58–60). In parallel, clinico-pathological studies strongly correlate pTau and NFT load with cognitive symptoms antemortem (1, 61, 62). From the epitopes evaluated here, pSer396/404 (PHF-1) inversely correlates with global cognitive scores and is a marker of more “matured” tangles, while pSer202 (CP13) and pSer202/ Thr205 (AT8) have been considered to recognize earlier NFTs, suggesting that β3-AR agonists can potentially modify tangles at different stages of development (60, 63). Such changes can potentially translate into better cognitive outcomes as we have previously reported that β3-AR agonist treatment reverses impaired object recognition memory in aged 3xTg-AD model (28). Furthermore, as plasma pTau-217 concentrations stand as the most promising fluid biomarker of AD pathology (30, 31), we tested whether it was detectable in this model and modulated by cold exposure and CL-316,243 pre-treatment. Although circulating pTau-217 levels remained low in this mouse model, cold exposure allowed us to quantify it and to show that the agonist partially reversed this cold-induced increase. Overall, considering the importance of tau phosphorylation on cognitive symptoms and as a biomarker of AD, the present results provide preclinical evidence supporting the prevention of pTau increases through modulation of BAT thermogenesis.

Mechanistic insights: The BAT-periphery-brain axis

Decades of work on neurocognitive disorders underscore that peripheral factors are closely intertwined with brain health and both must be considered as part of an integrated system (64). The observed impact of chronic treatment with a β3-AR agonist may be indirect, through a peripheral mechanism, and/or direct within the central nervous system. One central pathway involves improved glucose response and insulin sensitivity. Insulin resistance, both at the peripheral and cerebrovascular levels, has been associated with cognitive decline in AD (46, 65–67) and metabolic interventions aiming at improving these metabolic parameters have shown promising results in preclinical and clinical trials (38, 68).

A direct BAT-brain link may also stem the release of “batokines.” As a metabolic organ, BAT secretes hormones capable of exerting action in different tissues (22, 24, 26). Here, *fgf21* mRNA levels in the BAT were upregulated both in treated and saline-injected mice exposed to a cold challenge whereas circulating FGF21 was decreased following β3-AR activation. Similar results were observed in our previous study using repeated short cold exposures (17). Notably, we observed a strong association between circulating FGF21 levels and activation of the FGFR receptor in BAT. FGF21 may also target other tissues, such as liver and hypothalamus, to improve IR, thereby improving cognitive status. (69, 70). Thus, it is possible that BAT-derived molecular mediators, such as FGF21, exert an action both in the periphery and in the brain.

β3-AR distribution

Although the present work confirms the ability of β3-AR agonists to engage their targets in BAT, translation toward clinical application in humans requires careful consideration of the distribution of these receptors within the human body. While β3-AR mRNA has been detected in brain regions involved in cognitive function, including the hippocampus and cortex (71, 72), it remains unclear whether β3-AR agonists such as CL-316,243, or their potentially active metabolites, can cross the blood–brain barrier (73). Still, other β3-AR agonists such as the clinically used mirabegron and amibegron have shown to increase ^{18}F-FDG uptake in the prefrontal cortex and to have anxiolytic and antidepressive properties (74, 75). Regarding adipose tissue, exactly how much β3-AR is present in human brown adipocytes has risen translatability concerns. Nonetheless, analyses of human brown adipose tissue biopsies confirm the expression of β3-AR and thermogenic genes, including *ucp1*, which is associated with cardiometabolic health (76–80), while clinical interventions using the selective β3-AR agonist mirabegron demonstrate dose-dependent increases in BAT metabolic activity (81, 82). Although it remains uncertain whether BAT function in aged humans can be stimulated to the same extent as in old rodents, the emerging concept of a BAT–brain axis integrating metabolic, thermogenic, vascular, and enzymatic mechanisms represents a potentially pharmacologically targetable pathway, particularly when combined with lifestyle interventions, aimed at improving metabolic health and slowing AD progression.

Limitations

In this study, we used only males and thus could not evaluate any potential sex-differences. Female 3xTg-AD mice display an exacerbated metabolic and Aβ pathology compared to males and could potentially benefit more from the effects seen with the β3-AR agonist (36, 83). It would be interesting to confirm these results in female mice controlling for temperature variations due to the estrous cycle. Sample size was limited (n = < 7) for some measurements due to constraints in samples availability and ethical considerations, and thus these results should be interpreted with caution. In addition, it is important to acknowledge that rodents and humans differ in their thermogenic capacity (84). While rodents exhibit greater thermogenic capacity than humans, implying a more limited contribution of BAT in humans, recent studies show that WAT browning (beiging) occurs in humans and is linked to favorable metabolic outcomes (76–79). Hence, pharmacological interventions that specifically target

thermogenesis including sympathomimetics, β3-AR, and TRVP-1 agonists can counter these challenges by recruiting higher BAT volume and increasing its metabolic activity, even in older individuals (48).

Conclusions

The present work provides evidence that stimulation of the β3-AR in the BAT prevents the increase of cerebral and plasmatic pTau induced by a cold exposure in 3xTg-AD mice, in addition to beneficial impact on metabolic endpoints and Aβ neuropathology. This study further provides evidence for drug repurposing of β3-AR agonists in AD. BAT activation has primarily been evaluated for obesity and diabetes in phase I/II trials using the β3-AR agonist mirabegron (NCT04666636, NCT03012113, NCT02919176), and has shown modest effect sizes compared to more potent agents such as GLP-1 agonists (49, 50). However, in AD research the scenario is different as there are very few effective approved interventions and no convincing evidence of efficacy for GLP-1 agonists (85). Therefore, measurable effects, even if limited to certain patient subgroups, could still offer valuable therapeutic progress in age-related dementia.

Abbreviations

3xTg-AD
Triple transgenic mouse model of AD
β3-AR
β3 adrenergic receptor
Aβ
amyloid-β
AD
Alzheimer’s disease
Ago
β3-AR agonist (CL316,243)
AUC
Area under the curve
BACE-1
Beta- secretase 1
BAT
Brown adipose tissue
CV, CIV, CIII, CII, CI
Mitochondrial oxidative phosphorylation system complex V, IV, III, II, I
eEF2
Eukaryotic elongation factor 2
FGF21
Fibroblast growth factor-21
GTT

Glucose tolerance test
IDE
insulin degrading enzyme
ITT
insulin tolerance test
NonTg
Non-transgenic mice
OD
optical density
S
saline-treated mice
T°
temperature
UCP1
Uncoupling protein 1.

Declarations

Ethics approval and consent to participate

All animal experiments were performed in accordance with the Canadian Councial on animal Care and were approved by the Institutional Committee of the Centre Hospitalier de l'Université Laval (CHUL).

Consent for publication

Not applicable

Availability of data and materials

The datasets used and/ or analyzed during the current study are available from the corresponding author on reasonable request.

Competing interests

No competing interests

Funding

This research project was financially supported by grants to F.C. from the Alzheimer Society Canada (#20-01) and the Canadian Institutes of Health Research (PJT-183735 and PJT-168927). J.VE. was funded by scholarships from the faculty of pharmacy at Université Laval, Consortium for the Early Identification of Alzheimer's Disease- Québec (CIMA-Q), and Fonds de recherche du Québec-Santé (FRQS).

Author contributions

J. VE. Designed the study, performed animal experiments, drug administration, metabolic evaluations, protein extractions, Western blots, statistical analysis interpretation of the data and wrote the manuscript. H.D. contributed to RT-qPCR experiments. P.P. contributed to Western blots. M.T. participated to the conception of the study, provided expertise for thermoregulation and reviewed the manuscript. C.T. performed Aβ quantifications. V.E. read and review the manuscript. S.H. provided qPCR equipment, guidance and reviewed the manuscript. E.P. provided expertise for tau and reviewed the manuscript. F.C. secured funding, conceptualized and supervised the study and revised the manuscript. F.C. is the guarantor of this work and, as such, had full access to all the data in the study and takes responsibility for the integrity of the data and the accuracy of the data analysis. All authors reviewed and approved the final manuscript.

Acknowledgements

The authors thank the animal facility technicians Sonia Francoeur, Stéphanie Bernard and France Duclos for their help during the animal experiments.

References

1. Tremblay C, Pilote M, Phivilay A, Emond V, Bennet DA, Calon F. Biochemical characterization of Aβ and tau pathologies in Mild Cognitive Impairment and Alzheimer's Disease. J Alzheimer's Disease. 2007;12:377–90.
2. Alzheimer A, Stelzmann RA, Schnitzlein HN, Murtagh FR. An English translation of Alzheimer's 1907 paper, Uber eine eigenartige Erkankung der Hirnrinde. Clin Anat. 1995;8(6):429–31.
3. Hardy J, Selkoe DJ. The amyloid hypothesis of Alzheimer's disease:progress and problems on the road to therapeutics. Science. 2022;297:353–6.
4. Millyard A, Layden JD, Pyne D, Edwards A, Bloxham S. Impairments to Thermoregulation in the Elderly During Heat Exposure Events. Gerontol Geriatric Med. 2020;6.
5. Geneva II, Cuzzo B, Fazili T, Javaid W. Normal Body Temperature: A Systematic Review. Open Forum Infect Dis. 2019;6(4):ofz032.
6. Wildgoose C, Valenza A, Buoite Stella A, Feka K, Bianco A, Filingeri D. Ageing reduces skin wetness sensitivity across the body. Exp Physiol. 2021;106(12):2434–44.
7. Dhami P, Alagiakrishnan K. Approach to Low Body Temperature or Mild Hypothermia in the Geriatric Population: A Narrative Review. J Clin Med Res. 2026;18(4):219–33.
8. Holtzman A, Simon EW. Body temperature as a risk factor for Alzheimer's disease. Med Hypotheses. 2000;55(5):440–4.
9. Blessing EM, Parekh A, Betensky RA, Babb J, Saba N, Debure L, et al. Association between lower body temperature and increased tau pathology in cognitively normal older adults. Neurobiol Dis. 2022;171:105748.

10. Eggenberger P, Burgisser M, Rossi RM, Annaheim S. Body Temperature Is Associated With Cognitive Performance in Older Adults With and Without Mild Cognitive Impairment: A Cross-sectional Analysis. Front Aging Neurosci. 2021;13:585904.
11. Yamagiwa D, Katayama O, Yamaguchi R, Makino K, Shimada H. Association between Relative Hypothermia and Cognitive Function in Older Adults: A Cross-Sectional Study. J Am Med Dir Assoc. 2025;26(4):105472.
12. Canet G, Da Gama Monteiro F, Rocaboy E, Diego-Diaz S, Khelaifia B, Godbout K et al. Sleep-wake variation in body temperature regulates tau secretion and correlates with CSF and plasma tau. J Clin Invest. 2025.
13. Planel E, Bretteville A, Liu L, Virag L, Du AL, Yu WH, et al. Acceleration and persistence of neurofibrillary pathology in a mouse model of tauopathy following anesthesia. FASEB J. 2009;23(8):2595–604.
14. Vandal M, White PJ, Tournissac M, Tremblay C, St-Amour I, Drouin-Ouellet J, et al. Impaired thermoregulation and beneficial effects of thermoneutrality in the 3xTg-AD model of Alzheimer's disease. Neurobiol Aging. 2016;43:47–57.
15. Tournissac M, Leclerc M, Valentin-Escalera J, Vandal M, Bosoi CR, Planel E, et al. Metabolic determinants of Alzheimer's disease: A focus on thermoregulation. Ageing Res Rev. 2021;72:101462.
16. Gratuze M, El Khoury NB, Turgeon A, Julien C, Marcouiller F, Morin F, et al. Tau hyperphosphorylation in the brain of ob/ob mice is due to hypothermia: Importance of thermoregulation in linking diabetes and Alzheimer's disease. Neurobiol Dis. 2017;98:1–8.
17. Tournissac M, Bourassa P, Martinez-Cano RD, Vu TM, Hebert SS, Planel E, et al. Repeated cold exposures protect a mouse model of Alzheimer's disease against cold-induced tau phosphorylation. Mol Metab. 2019;22:110–20.
18. Tournissac M, Vandal M, Francois A, Planel E, Calon F. Old age potentiates cold-induced tau phosphorylation: linking thermoregulatory deficit with Alzheimer's disease. Neurobiol Aging. 2017;50:25–9.
19. El Khoury NB, Gratuze M, Petry F, Papon MA, Julien C, Marcouiller F, et al. Hypothermia mediates age-dependent increase of tau phosphorylation in db/db mice. Neurobiol Dis. 2016;88:55–65.
20. Planel E, Miyasaka T, Launey T, Chui DH, Tanemura K, Sato S, et al. Alterations in glucose metabolism induce hypothermia leading to tau hyperphosphorylation through differential inhibition of kinase and phosphatase activities: implications for Alzheimer's disease. J Neurosci. 2004;24(10):2401–11.
21. Brum WS, Montoliu-Gaya L, Brinkmalm G, Piotrowska D, Camporesi E, Jager C, et al. Reversible tau hyperphosphorylation in hibernation: a blood biomarker and brain tissue study. Acta Neuropathol. 2025;150(1):36.
22. Cypess AM, Cannon B, Nedergaard J, Kazak L, Chang DC, Krakoff J, et al. Emerging debates and resolutions in brown adipose tissue research. Cell Metab. 2025;37(1):12–33.

23. Virtanen KA, Lidell ME, Orava J, Heglind M, Westergren R, Niemi T, et al. Functional Brown Adipose Tissue in Healthy Adults. NEJM. 2009;360:1518–25.
24. Carpentier AC, Blondin DP, Haman F, Richard D. Brown Adipose Tissue-A Translational Perspective. Endocr Rev. 2023;44(2):143–92.
25. Cypess AM, Lehman S, Williams G, Tal I, Rodman D, Goldfine AB, et al. Identification and Importance of Brown Adipose Tissue in Adult Humans. NEJM. 2009;360:1509–17.
26. Becher T, Palanisamy S, Kramer DJ, Eljalby M, Marx SJ, Wibmer AG, et al. Brown adipose tissue is associated with cardiometabolic health. Nat Med. 2021;27(1):58–65.
27. Tabuchi C, Sul HS. Signaling Pathways Regulating Thermogenesis. Front Endocrinol (Lausanne). 2021;12:595020.
28. Tournissac M, Vu TM, Vrabic N, Hozer C, Tremblay C, Melancon K, et al. Repurposing beta-3 adrenergic receptor agonists for Alzheimer's disease: beneficial effects in a mouse model. Alzheimers Res Ther. 2021;13(1):103.
29. Feng Q, Cheng B, Yang R, Sun FY, Zhu CQ. Dynamic changes of phosphorylated tau in mouse hippocampus after cold water stress. Neurosci Lett. 2005;388(1):13–6.
30. Ashton NJ, Brum WS, Di Molfetta G, Benedet AL, Arslan B, Jonaitis E, et al. Diagnostic Accuracy of a Plasma Phosphorylated Tau 217 Immunoassay for Alzheimer Disease Pathology. JAMA Neurol. 2024;81(3):255–63.
31. Teunissen CE, Kolster R, Triana-Baltzer G, Janelidze S, Zetterberg H, Kolb HC. Plasma p-tau immunoassays in clinical research for Alzheimer's disease. Alzheimers Dement. 2025;21(1):e14397.
32. Tremblay C, Francois A, Delay C, Freland L, Vandal M, Bennett DA, et al. Association of Neuropathological Markers in the Parietal Cortex With Antemortem Cognitive Function in Persons With Mild Cognitive Impairment and Alzheimer Disease. J Neuropathol Exp Neurol. 2017;76(2):70–88.
33. Cummings JL, Zhou Y, Yang Y, Zhong K, Fonseca J, Osse AL et al. Alzheimer's disease drug development pipeline: 2026. Alzheimers Dement (N Y). 2026;12:e70251.
34. Cintron-Colon R, Shankar K, Sanchez-Alavez M, Conti B. Gonadal hormones influence core body temperature during calorie restriction. Temp (Austin). 2019;6(2):158–68.
35. Swift KM, Gary NC, Urbanczyk PJ. On the basis of sex and sleep: the influence of the estrous cycle and sex on sleep-wake behavior. Front Neurosci. 2024;18:1426189.
36. Vandal M, White PJ, Chevrier G, Tremblay C, St-Amour I, Planel E, et al. Age-dependent impairment of glucose tolerance in the 3xTg-AD mouse model of Alzheimer's disease. FASEB J. 2015;29(10):4273–84.
37. Canet G, Rocaboy E, Laliberte F, Boscher E, Guisle I, Diego-Diaz S, et al. Temperature-induced Artifacts in Tau Phosphorylation: Implications for Reliable Alzheimer's Disease Research. Exp Neurobiol. 2023;32(6):423–40.

38. Vandal M, White PJ, Tremblay C, St-Amour I, Chevrier G, Emond V, et al. Insulin reverses the high-fat diet-induced increase in brain Abeta and improves memory in an animal model of Alzheimer disease. Diabetes. 2014;63(12):4291–301.
39. Natarajan D, Plakkot B, Tiwari K, Ekambaram S, Wang W, Rudolph M et al. Chronic beta3-AR stimulation activates distinct thermogenic mechanisms in brown and white adipose tissue and improves systemic metabolism in aged mice. Aging Cell. 2024:e14321.
40. Medak KD, McKie GL, Shamshoum H, Seguin I, Wright DC. The glucose lowering effects of CL 316,243 dissipate with repeated use and are rescued bycilostamide. Physiol Rep. 2022;10(4):e15187.
41. Michel MC. Do β-adrenoceptor agonists induce homologous or heterologous desensitization in rat urinary bladder? Naunyn Schmiedebergs Arch Pharmacol. 2014;387(3):215–24.
42. Nam M, Cooper MP. Role of Energy Metabolism in the Brown Fat Gene Program. Front Endocrinol (Lausanne). 2015;6:104.
43. Queathem ED, Welly RJ, Clart LM, Rowles CC, Timmons H, Fitzgerald M et al. White Adipose Tissue Depots Respond to Chronic Beta-3 Adrenergic Receptor Activation in a Sexually Dimorphic and Depot Divergent Manner. Cells. 2021;10(12).
44. Livingston G, Huntley J, Liu KY, Costafreda SG, Selbaek G, Alladi S, et al. Dementia prevention, intervention, and care: 2024 report of the Lancet standing Commission. Lancet. 2024;404(10452):572–628.
45. Kellar D, Craft S. Brain insulin resistance in Alzheimer's disease and related disorders: mechanisms and therapeutic approaches. Lancet Neurol. 2020;19(9):758–66.
46. Rhea EM, Leclerc M, Yassine HN, Capuano AW, Tong H, Petyuk VA, et al. State of the Science on Brain Insulin Resistance and Cognitive Decline Due to Alzheimer's Disease. Aging Dis. 2024;15(4):1688–725.
47. Finlin BS, Memetimin H, Zhu B, Confides AL, Vekaria HJ, El Khouli RH, et al. The beta3-adrenergic receptor agonist mirabegron improves glucose homeostasis in obese humans. J Clin Invest. 2020;130(5):2319–31.
48. O'Mara AE, Johnson JW, Linderman JD, Brychta RJ, McGehee S, Fletcher LA, et al. Chronic mirabegron treatment increases human brown fat, HDL cholesterol, and insulin sensitivity. J Clin Invest. 2020;130(5):2209–19.
49. Hegland TA, Fang Z, Bucher K. GLP-1 Medication Use for Type 2 Diabetes Has Soared. JAMA. 2024;332(12):952–3.
50. Watanabe JH, Kwon J, Nan B, Reikes A. Trends in glucagon-like peptide 1 receptor agonist use, 2014 to 2022. J Am Pharm Assoc (2003). 2024;64(1):133-8.
51. Rolstad S, Berg AI, Bjerke M, Blennow K, Johansson B, Zetterberg H, et al. Amyloid-beta(4)(2) is associated with cognitive impairment in healthy elderly and subjective cognitive impairment. J Alzheimers Dis. 2011;26(1):135–42.

52. Bennett DA, Schneider JA, Wilson RS, Bienias JL, Arnold SE. Neurofibrillary tangles mediate the association of amyloid load with clinical Alzheimer disease and level of cognitive function. Arch Neurol. 2004;61(3):378–84.
53. Perneczky R, Dom G, Chan A, Falkai P, Bassetti C. Anti-amyloid antibody treatments for Alzheimer's disease. Eur J Neurol. 2023;31(2).
54. Hoy SM, Lecanemab. First Approval Drugs. 2023;83(4):359–65.
55. Arber C, Villegas-Llerena C, Toombs J, Pocock JM, Ryan NS, Fox NC, et al. Amyloid precursor protein processing in human neurons with an allelic series of the PSEN1 intron 4 deletion mutation and total presenilin-1 knockout. Brain Commun. 2019;1(1):fcz024.
56. Petit D, Fernandez SG, Zoltowska KM, Enzlein T, Ryan NS, O'Connor A, et al. Abeta profiles generated by Alzheimer's disease causing PSEN1 variants determine the pathogenicity of the mutation and predict age at disease onset. Mol Psychiatry. 2022;27(6):2821–32.
57. Oddo S, Caccamo A, Shepherd JD, Murphy MP, Golde TE, Kayed R, et al. Triple-transgenic model of Alzheimer's disease with plaques and tangles: intracellular Abeta and synaptic dysfunction. Neuron. 2003;39(3):409–21.
58. Dujardin S, Commins C, Lathuiliere A, Beerepoot P, Fernandes AR, Kamath TV, et al. Tau molecular diversity contributes to clinical heterogeneity in Alzheimer's disease. Nat Med. 2020;26(8):1256–63.
59. Colom-Cadena M, Davies C, Sirisi S, Lee J-E, Simzer EM, Tzioras M et al. Synaptic oligomeric tau in Alzheimer’s disease — A potential culprit in the spread of tau pathology through the brain. Neuron. 2023;111(14):2170-83.e6.
60. Koss DJ, Jones G, Cranston A, Gardner H, Kanaan NM, Platt B. Soluble pre-fibrillar tau and beta-amyloid species emerge in early human Alzheimer's disease and track disease progression and cognitive decline. Acta Neuropathol. 2016;132(6):875–95.
61. Murray ME, Moloney CM, Kouri N, Syrjanen JA, Matchett BJ, Rothberg DM, et al. Global neuropathologic severity of Alzheimer's disease and locus coeruleus vulnerability influences plasma phosphorylated tau levels. Mol Neurodegener. 2022;17(1):85.
62. Jack CR Jr., Bennett DA, Blennow K, Carrillo MC, Dunn B, Haeberlein SB, et al. NIA-AA Research Framework: Toward a biological definition of Alzheimer's disease. Alzheimers Dement. 2018;14(4):535–62.
63. Moloney CM, Lowe VJ, Murray ME. Visualization of neurofibrillary tangle maturity in Alzheimer's disease: A clinicopathologic perspective for biomarker research. Alzheimers Dement. 2021;17(9):1554–74.
64. Goncalves RA, De Felice FG. The crosstalk between brain and periphery: Implications for brain health and disease. Neuropharmacology. 2021;197:108728.
65. Leclerc M, Bourassa P, Tremblay C, Caron V, Sugere C, Emond V, et al. Cerebrovascular insulin receptors are defective in Alzheimer's disease. Brain. 2023;146(1):75–90.
66. Biswas R, Capuano AW, Mehta RI, Barnes LL, Bennett DA, Arvanitakis Z. Review of Associations of Diabetes and Insulin Resistance With Brain Health in Three Harmonised Cohort Studies of Ageing

and Dementia. Diabetes Metab Res Rev. 2025;41(1):e70032.
67. Kim AB, Arvanitakis Z. Insulin resistance, cognition, and Alzheimer disease. Obes (Silver Spring). 2023;31(6):1486–98.
68. Erichsen J, Craft S. Targeting immunometabolic pathways for combination therapy in Alzheimer's disease. Alzheimers Dement (N Y). 2023;9(4):e12423.
69. Geng L, Lam KSL, Xu A. The therapeutic potential of FGF21 in metabolic diseases: from bench to clinic. Nat Rev Endocrinol. 2020;16(11):654–67.
70. Kliewer SA, Mangelsdorf DJ. A Dozen Years of Discovery: Insights into the Physiology and Pharmacology of FGF21. Cell Metab. 2019;29(2):246–53.
71. Summers RJ, Papaioannou M, Harris S, Evans BA. Expression of beta 3-adrenoceptor mRNA in rat brain. Br J Pharmacol. 1995;116(6):2547–8.
72. Rodriguez M, Carillon C, Coquerel A, Le Fur G, Ferrara P, Caput D et al. Evidence for the presence of beta 3-adrenergic receptor mRNA in the human brain. Mol Brain Res. 1995;29(2).
73. Mirbolooki MR, Schade KN, Constantinescu CC, Pan ML, Mukherjee J. Enhancement of 18F-fluorodeoxyglucose metabolism in rat brain frontal cortex using a beta3 adrenoceptor agonist. Synapse. 2015;69(2):96–8.
74. Stemmelin J, Cohen C, Terranova JP, Lopez-Grancha M, Pichat P, Bergis O, et al. Stimulation of the beta3-Adrenoceptor as a novel treatment strategy for anxiety and depressive disorders. Neuropsychopharmacology. 2008;33(3):574–87.
75. Claustre Y, Leonetti M, Santucci V, Bougault I, Desvignes C, Rouquier L, et al. Effects of the beta3-adrenoceptor (Adrb3) agonist SR58611A (amibegron) on serotonergic and noradrenergic transmission in the rodent: relevance to its antidepressant/anxiolytic-like profile. Neuroscience. 2008;156(2):353–64.
76. Loft A, Emont MP, Weinstock A, Divoux A, Ghosh A, Wagner A, et al. Towards a consensus atlas of human and mouse adipose tissue at single-cell resolution. Nat Metab. 2025;7(5):875–94.
77. Tran KV, Brown EL, DeSouza T, Jespersen NZ, Nandrup-Bus C, Yang Q, et al. Human thermogenic adipocyte regulation by the long noncoding RNA LINC00473. Nat Metab. 2020;2(5):397–412.
78. Jespersen NZ, Feizi A, Andersen ES, Heywood S, Hattel HB, Daugaard S, et al. Heterogeneity in the perirenal region of humans suggests presence of dormant brown adipose tissue that contains brown fat precursor cells. Mol Metab. 2019;24:30–43.
79. Vijay J, Gauthier MF, Biswell RL, Louiselle DA, Johnston JJ, Cheung WA, et al. Single-cell analysis of human adipose tissue identifies depot and disease specific cell types. Nat Metab. 2020;2(1):97–109.
80. Cero C, Lea HJ, Zhu KY, Shamsi F, Tseng YH, Cypess AM. beta3-Adrenergic receptors regulate human brown/beige adipocyte lipolysis and thermogenesis. JCI Insight. 2021;6(11).
81. Cypess AM, Weiner LS, Roberts-Toler C, Franquet Elia E, Kessler SH, Kahn PA, et al. Activation of human brown adipose tissue by a beta3-adrenergic receptor agonist. Cell Metab. 2015;21(1):33–8.

82. Dumont L, Caron A, Richard G, Croteau E, Fortin M, Frisch F, et al. The effects of the beta(1)-adrenergic receptor antagonist bisoprolol administration on mirabegron-stimulated human brown adipose tissue thermogenesis. Acta Physiol (Oxf). 2024;240(5):e14127.
83. Hirata-Fukae C, Li HF, Hoe HS, Gray AJ, Minami SS, Hamada K, et al. Females exhibit more extensive amyloid, but not tau, pathology in an Alzheimer transgenic model. Brain Res. 2008;1216:92–103.
84. Skop V, Guo J, Liu N, Xiao C, Hall KD, Gavrilova O, et al. Mouse Thermoregulation: Introducing the Concept of the Thermoneutral Point. Cell Rep. 2020;31(2):107501.
85. Cummings JL, Atri A, Sano M, Zetterberg H, Scheltens P, Knop FK et al. Efficacy and safety of oral semaglutide 14 mg (flexible dose) in early-stage symptomatic Alzheimer's disease (evoke and evoke+): two phase 3, randomised, placebo-controlled trials. Lancet. 2026.

Figures

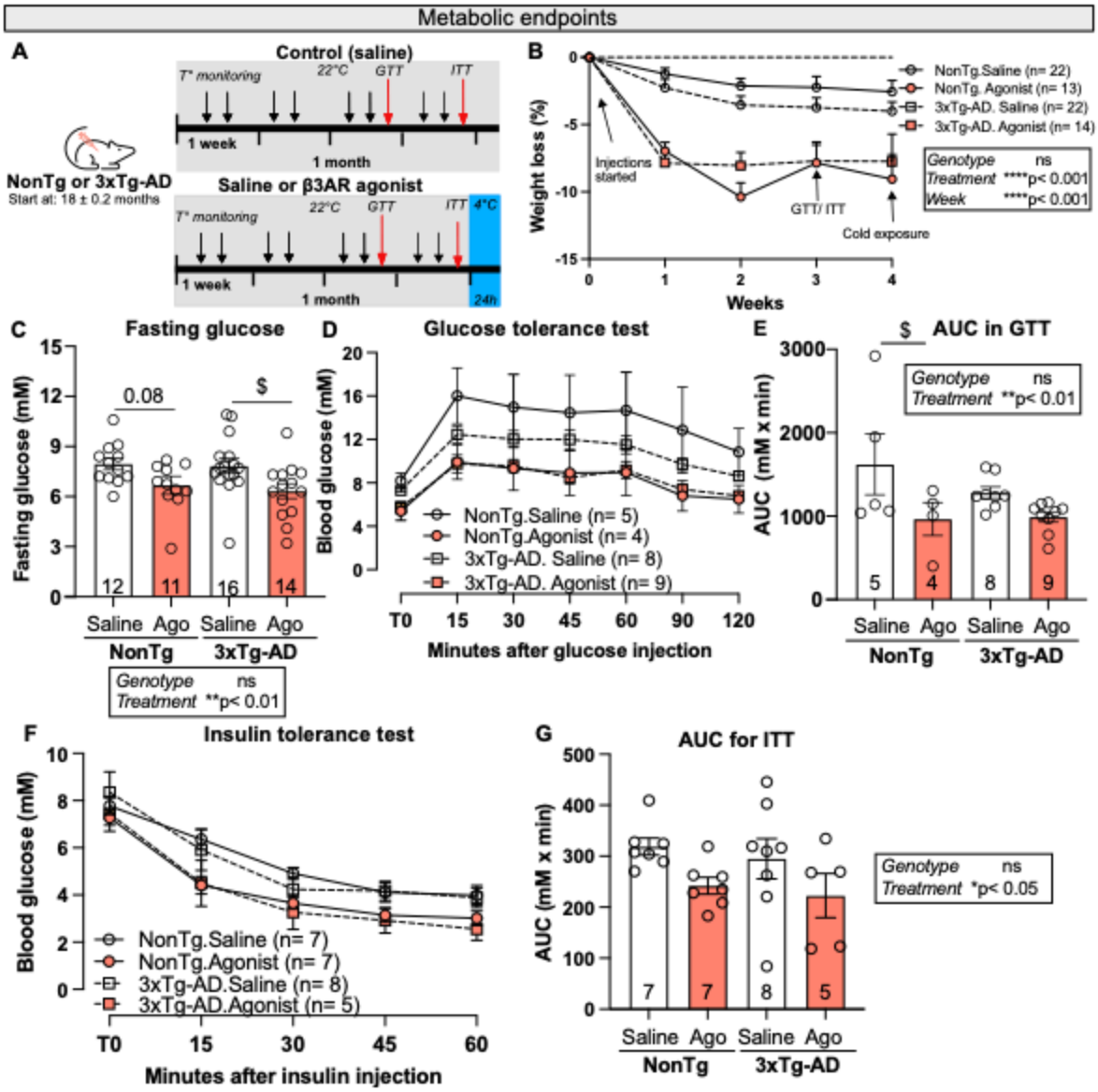


Figure 1

b3-AR stimulation improves peripheral glucose and insulin metabolism in NonTg and 3xTg-AD mice. **A)** Schematic of the animal protocol: 18-month-old 3xTg-AD and NonTg mice received saline or a b3-AR agonist (CL-316,243, 1mg/kg, i.p.) daily for a month at room temperature, before undergoing a 24-hour cold challenge (4°C). **B)** Body weight loss (% change from baseline) during the four weeks of treatment. **C)** Blood glucose (mM) in 6-hour fasted mice measured before ITT and GTT. **D**) Glucose tolerance test (GTT) consisted in measuring blood glucose at consistent intervals for 2 hours in fasted mice (6 h) after the injection of a bolus of glucose (1g/ kg i.p.) on the third week of treatment and **E)** area under the curve for GTT. **F)** Insulin tolerance test (ITT) consisted in measuring blood glucose for 1 hour in fasted mice (6 h) after an injection of a bolus of insulin (1 U/kg, i.p.) on the fourth week of treatment and **G)** area under the curve for ITT. Blood glucose was measured using a glucometer. Data are presented as mean ± SEM (n/group indicated in graphs). *Statistics:* **B)** Repeated-measures ANOVA (mixed-effect model) with week as the within-subject factor and genotype and treatment as fixed effects: effect of genotype ns; effect of treatment ****p< 0.0001. **C, E, G)** Two-way ANOVA (shown on graphs), Šidák´s post-hoc ($^{\$}$p< 0.05). *Abbreviations*: 3xTg-AD: Triple transgenic mice; Ago: b3AR agonist-treated mice; S: saline-treated mice.

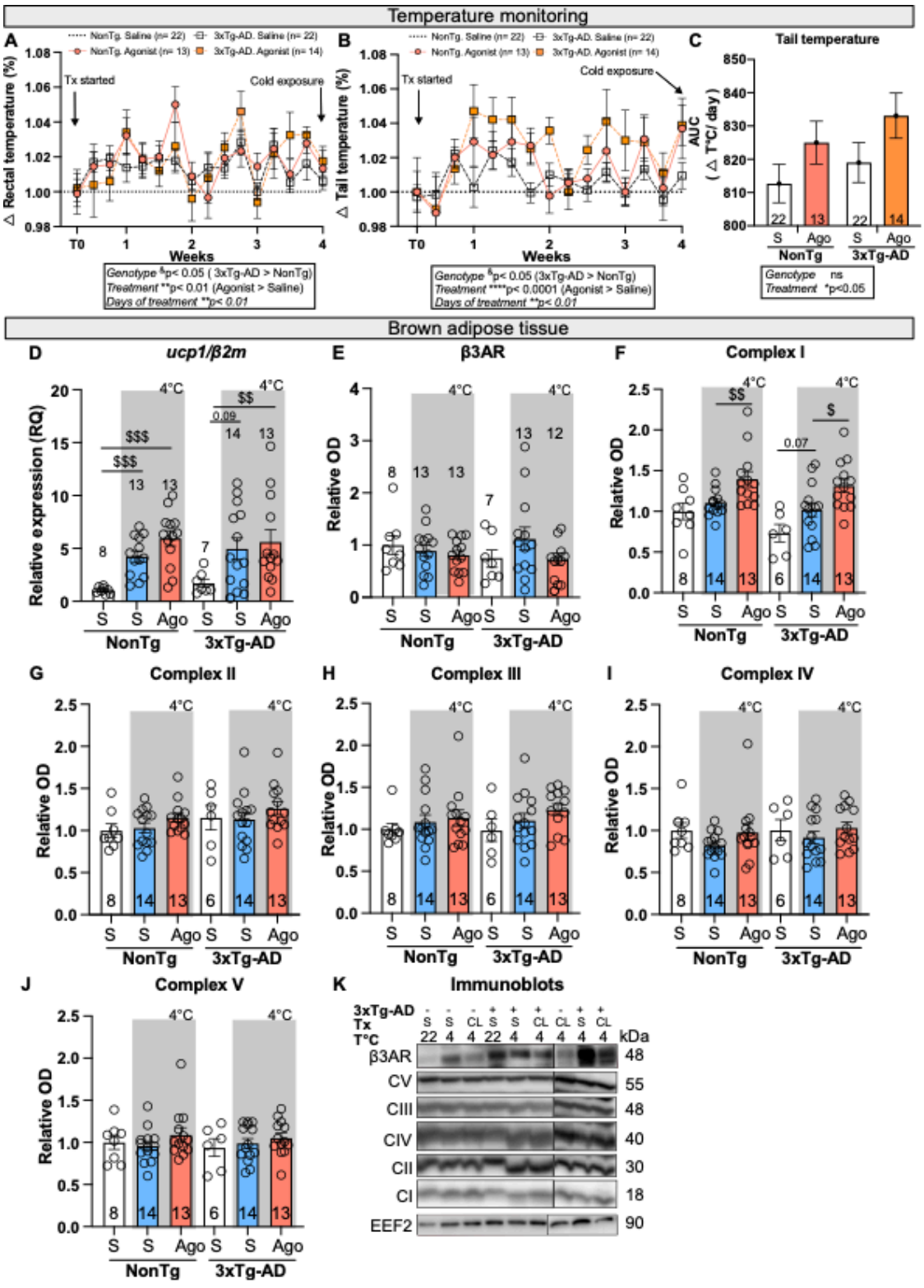


Figure 2

b3-AR stimulation followed by acute cold exposure increases thermogenesis in NonTg and 3xTg-AD mice. **A, B**) % change in rectal and IR temperature compared to NonTg-saline mice measured on alternate days during the 4-week treatment. **C)** AUC for IR temperature measured in the tail before i.p. injections. **D**) *ucp1/ β2m gene* expression in BAT. **E**) Relative β3-AR and **F-J**) mitochondrial oxidative phosphorylation proteins (CI-CV) measured by WB on BAT homogenates of NonTg and 3xTg-AD mice. **K**)

Examples of Western blots in BAT samples. Equal amounts of protein from each homogenate were loaded and run on the same gel in a randomized order. Thus, consecutive bands could not always be shown as examples. If the image has been cut to match the histogram, it in represented with a bold line. Values were normalized with total protein content. Data are presented as mean ± SEM (n/group indicated in each column). *Statistics*: **A, B**) Repeated-measures ANOVA (mixed effect model) with day as the within-subject factor and genotype and treatment as fixed effects: effect of genotype $^{\&}$p<0.05; effect of treatment **p< 0.01, ***p< 0.001. **C)** Two-way ANOVA (shown on graph); effect of genotype ns, effect of treatment *p<0.05. **D-J)** Kruskal-Wallis, followed by Wilcoxon's post hoc ($^{\$}$p< 0.05, $^{\$\$}$p< 0.01, $^{\$\$\$}$p< 0.001). *Abbreviations*: 3xTg-AD: Triple transgenic mice; Ago, CL: b3AR agonist CL-316,243; BAT: Brown adipose tissue; UCP1: Uncoupling protein 1; b2M: b2microglobulin; b3AR: b3 adrenergic receptor; NonTg: Non-transgenic; S: Saline-injected mice.

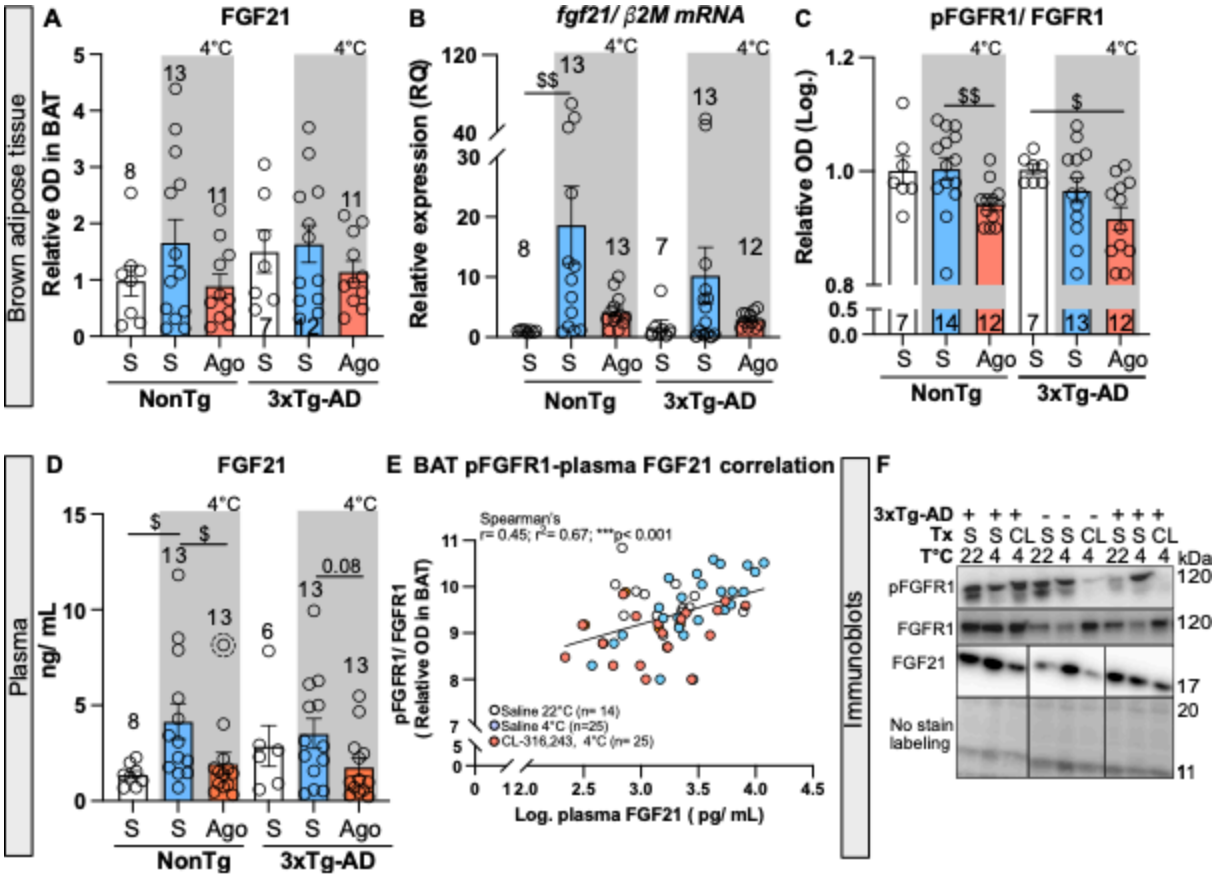


Figure 3

Cold exposure increases BAT and plasma FGF21, while β3-AR lowers FGFR1 in BAT. A) Relative FGF21 protein levels, **B**) *fgf21/b2m* mRNA gene expression measured by qPCR and **C**) relative pFGFR1 (Y216)/ FGFR1 ratio measured by WB in BAT homogenates. **D)** Plasma levels of murine FGF21 taken by intracardiac punction after acute cold exposure (4°C, 24h) and before sacrifice, **E**) Spearman's correlation between circulating FGF21 and pFGFR1/ FGFR1 ratio in BAT**, F)** Examples of Western blots. Equal amounts of protein from each homogenate were loaded and run on the same gel in a randomized order. Thus, consecutive bands could not always be shown as examples. If the image has been cut to

match the histogram, it is represented with a bold line. WB values were normalized with total protein content. Data are represented as mean ± SEM (n/group indicated in each column). *Statistics*: **A-D**) Kruskal-Wallis, followed by Wilcoxon's post hoc ($^{\$}p< 0.05$, $^{\$\$}p< 0.01$, $^{\$\$\$}p< 0.001$). *Abbreviations*: 3xTg-AD: Triple transgenic mice; Ago, CL: b3AR agonist CL-316,243; BAT: Brown adipose tissue; UCP1: Uncoupling protein 1; b2M: b2-microglobulin; b3AR: b3-adrenergic receptor; *fgf21*, FGF21: Fibroblast growth factor- 21; NonTg: Non- transgenic; S: Saline-injected mice.

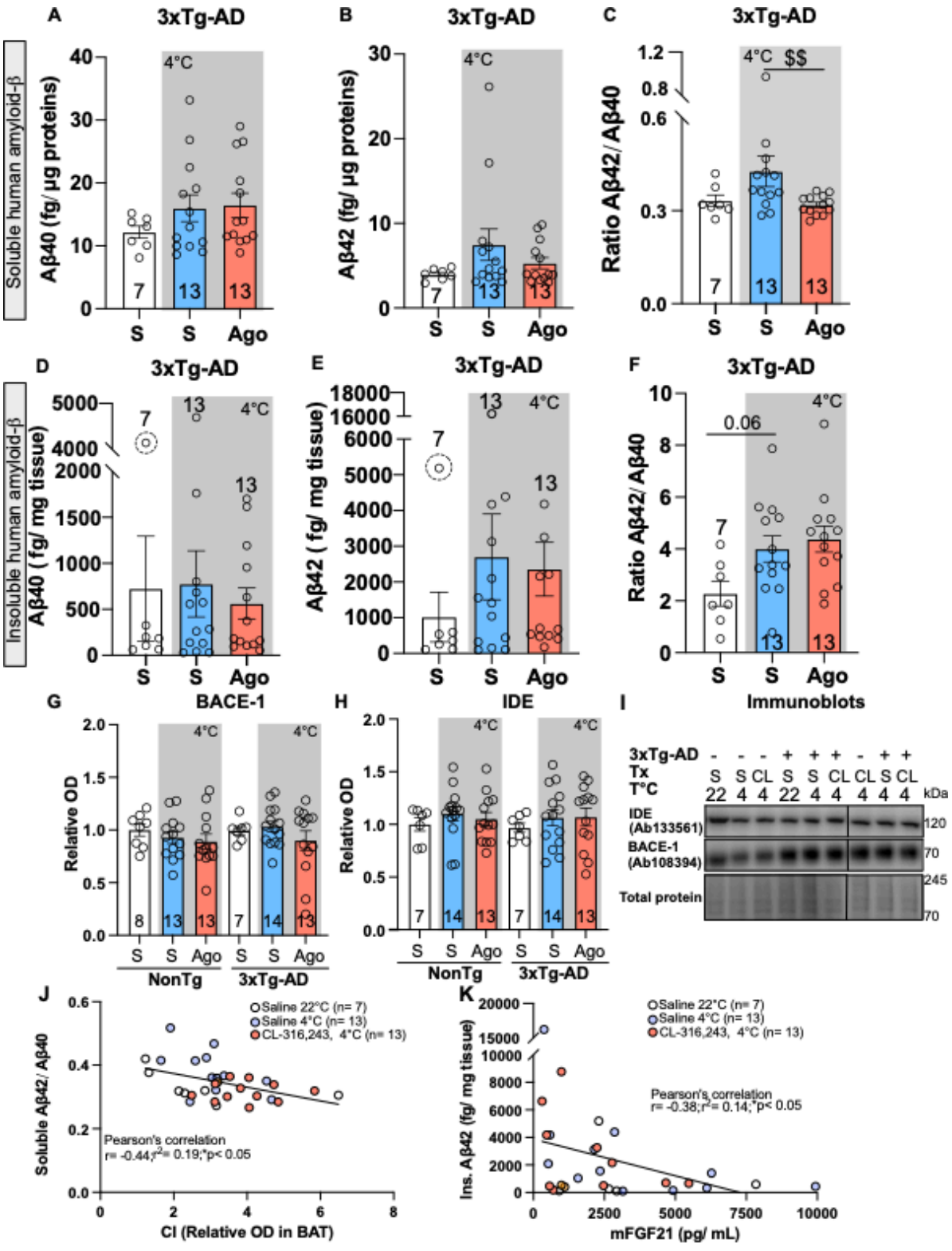


Figure 4

b3-AR maintains the soluble Ab42/Ab40 ratio at control levels in the cortex of cold-exposed 3xTg-AD mice. **A, B**) Human Ab40 and Ab42 peptides measured by ELISA in the TBS-soluble and in the **D, E**) detergent-insoluble fractions of cortex homogenates of 3xTg-AD mice, respectively. **C**) Ab42/Ab40 ratio of TBS-soluble and **F**) detergent-insoluble peptides in the cortex. **G, H**) Relative levels of BACE-1 and IDE shown as fold change in detergent-soluble homogenates and were normalized by total protein content. **I**) Examples of Western blots. Equal amounts of protein from each homogenate were loaded and run on the same gel in a randomized order. When bands were rearranged to match the histogram order, this is indicated by a dividing line. Data are presented as mean ± SEM (n/group indicated in each column). *Statistics*: Kruskal-Wallis, followed by Wilcoxon's post hoc test ($^{\$\$}p< 0.01$)**. J, K**) Pearson's correlations (*p< 0.05). *Abbreviations*: 3xTg-AD: triple transgenic mice; Ab: amyloid-b: Ago; b3AR agonist CL-316,243-injected group; BACE-1: β-site amyloid precursor protein cleaving enzyme 1; CI; Complex I (NADH: Ubiquinone oxidoreductase) from the mitochondrial oxidative phosphorylation system; IDE: Insulin-degrading enzyme; Ins: detergent- insoluble fraction; S: saline-injected group.

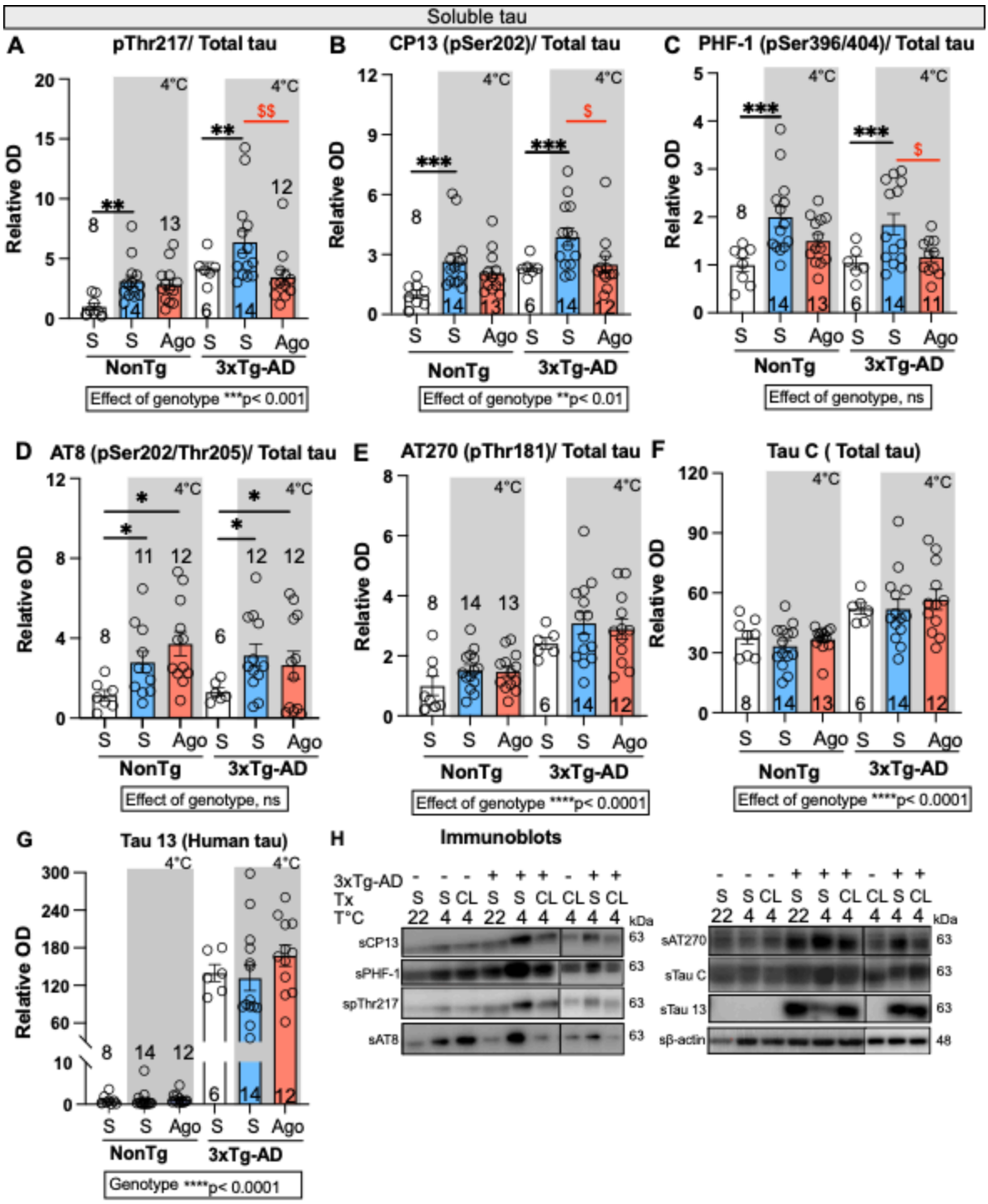


Figure 5

b3-AR stimulation prevents the hypothermia-induced rise in hippocampal pTau. A-E) Relative levels of the ratio pTau/total tau (Tau C) **F)** total human and mouse tau and **G)** total human tau measured in detergent soluble fractions of hippocampus homogenates of non-transgenic and 3xTg-AD mice. **H**) Examples of Western blots. Equal amounts of protein from each homogenate were loaded and run on the same gel in a randomized order. When bands were rearranged to match the histogram order, this is indicated by a dividing line. Data are represented as mean ± SEM (n/group indicated in each column). *Statistics*: **A-G)** Standard least square model with genotype and condition (saline 22°C, saline 4°C, and

agonist 4°C) as fixed effects, including their interaction; Dunnett's post-hoc with saline 22°C as the reference group (*p< 0.05, **p< 0.01). **A-G**) Kruskal-Wallis, followed by Wilcoxon's post hoc ($p< 0.05, $$p< 0.01, $$$p< 0.001, shown in red). Abbreviations: 3xTg-AD: Triple transgenic mice; Ago, CL: b3AR agonist CL-316,243; NonTg: Non-transgenic; S: Saline-injected mice.

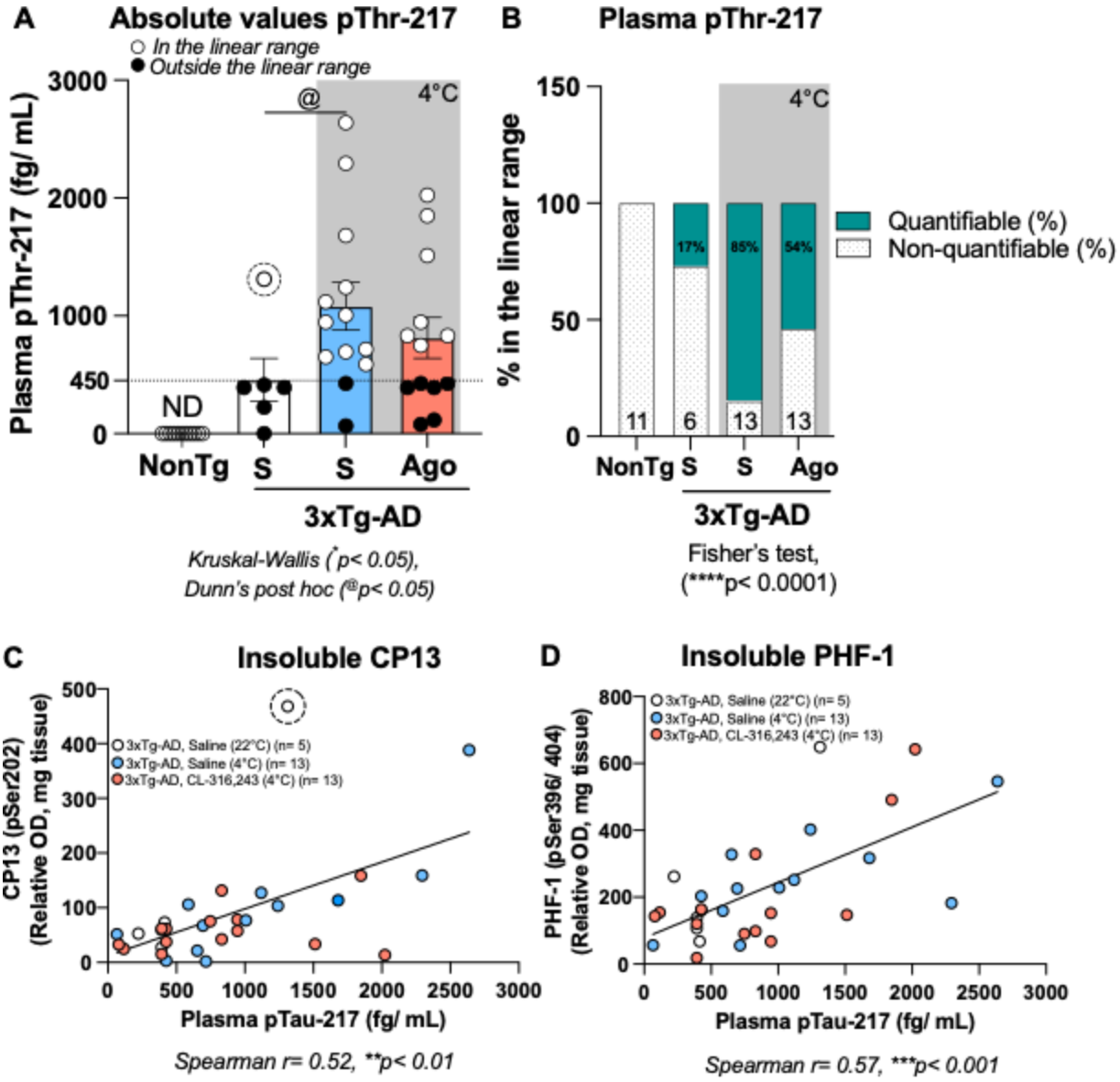


Figure 6

Cold exposure enables plasma pTau-217 detection, which is partially blocked by the b3-AR agonist pretreatment. A) Human pTau (pThr-217) levels (fg/mL) and **B**) % within the quantifiable range of pThr-217 in plasma taken before euthanasia, after mice were exposed at 4°C or left at room temperature and treated with CL316,243 or saline. Correlations between blood pTau217 (fg/mL) and **C)** insoluble CP13 and **D)** PHF-1 relative levels of 3xTg-AD mice only. Data are represented as mean ± SEM. *Statistics*: **A)** Kruskal-Wallis, followed by Dunn's post hoc (@p< 0.05). Circled outlier was excluded from analysis (ROUT method RQ= 1%). **B**) Contingency Fisher's exact test (****p< 0.0001) where NonTg values (non-detected) were not considered in the analysis. **C, D**) Spearman's correlations (**p< 0.01, ***p< 0.001).

Abbreviations: 3xTg-AD: Triple transgenic mice; Ago, CL: b3AR agonist CL-316,243; ND: Non-detected; NonTg: Non-transgenic; S: Saline-injected mice.

Supplementary Files

This is a list of supplementary files associated with this preprint. Click to download.

- Additionalfile1.Listofanitbodies.AlzRes.Ther.xlsx
- Additionalfile2AlzRes.Ther..ThermoMore.docx
- Additionalfile3.Blots.AlzRes.Ther..JV.docx